IFUSP/P-94

ANGULAR DISTRIBUTION OF FISSION FRAGMENTS FOLLOWING ELECTROEXCITATION**

by

D.S.Onley

Department of Physics, Ohio University,

Athens, Ohio - 45701, USA

and

B.S.Bhandari

Instituto de Física, Universidade de São Paulo

São Paulo,Brasil

** Work supported in part by FAPESP, FINEP and CNPq, Brasil.

ABSTRACT

The angular distribution of fission fragments following excitation by electron scattering is investigated using the method of the virtual photon spectrum, and the transition state hypothesis; the results are compared with photofission. Due to the lack of a strong selection rule on changes in the magnetic quantum number, electrons will not produce such pronounced angular distributions as photons. Sample calculations for energies around the ^{238}U threshold show that angular distributions should be appreciable nevertheless, particularly for quadrupole absorption. The possibility of using information from both photofission and electrofission for a more complete analysis, is discussed.

INTRODUCTION

The angular distribution of fragments resulting from nuclear fission following excitation by photons or fast neutrons, is known to be anisotropic in certain circumstances. Several years ago, A. Bohr[1] suggested that such anisotropies could be explained as a correlation between the angular distribution of emitted fragments and the quantum numbers of the nuclear transition state. Circumstances restricting the number of transition states accessible, or strongly favoring one particular state, would then lead to a characteristic angular distribution. These ideas have been discussed in more detail by Griffin[2] and further extended and used in analysis of angular distributions by many authors; useful summaries of current ideas may be found in reviews by Huizenga and coauthors[3-6].

Our purpose here is to investigate whether anisotropic angular distributions could be expected following fission induced by electron scattering, since this method has gained some attention in recent years[7-10]. We first give a very short review of the current ideas on the likely properties of the nuclear transition state, sufficient to justify the particular choices of energies and angular momenta for later examples. We formulate the spectrum of virtual photons emitted by the scattering electron and examine its dependence on the quantum numbers of angular momentum L,M, transferred between electron and nucleus. The details of calculation of the virtual photon spectrum for high Z targets has been given in an earlier paper by Gargaro and Onley[11] and our discussion of theory here will be limited to those aspects of the spectrum which determine the angular distributions of outgoing fragments (particularly the z-component of transferred angular momentum).

THE TRANSITION STATE

The transition state is supposed to describe the condition of the nucleus at a point just before fission, when the system is passing the highest point of the fission barrier(the outerbarrier if there is more than one[6]). If the energy imparted to the nucleus is barely above the threshold for surmounting this barrier, most of its energy is, at this point, invested in deformation, leaving the other degrees of freedom in a condition presumably very similar to that describing the lowest energy states of an extremely deformed nucleus. Aside from the quantum numbers L,M, of the nuclear angular momentum (which are of course well defined and conserved throughout the fission process), one may attempt to classify states into rotational bands, using the quantum number K (the projection of the angular momentum on the nuclear symmetry axis). Unlike L and M, the existence of a definable K is not guaranteed but is part of the transition state hypothesis. Supposing that the direction of emission of the fission fragments to be along the direction defined before fission by the nuclear symmetry axis, and supposing that subsequent emission of neutrons will not materially disturb this, then the angular distribution of emitted fragments is given by the probability distribution of the angles defining the original symmetry axis, i.e. by the square of the wavefunction for a symmetric top :

$$W^{L}_{MK}(\theta) = \left(\frac{2L+1}{2}\right) \cdot \left| d^{L}_{MK}(\theta) \right|^2 \qquad (1)$$

The notation and definition of d^{L}_{MK} used in ref.(6) are adopted here.

The functions of θ given by eq.(1) are quite

distinct for different values of L, M and K, but analysis of angular distributions can only be made, with any reliability, when the number of accessible states is very small. It is also necessary that the excitation mechanism does not populate all M-substates equally, since this would destroy the angular distributions even for an unique K and L. For photofission this condition is met very well, because angular momentum transfers are limited to magnetic substates with $M = \pm 1$.

A simple case to consider is the fission of an even-even nucleus such as ^{238}U. The strong inhibition of high angular momentum transfers in photoexcitation would justify considering $L^{\Pi} = 1^-$ as the prime candidate for the spin and parity of the excited state, with 2^+ and 1^+ as possible contenders. For transitions just above the barrier the most likely quantum numbers for rotational bands have been discussed by Huizenga[3] and are reproduced in fig.1. We can see that for energy very close to the top of the barrier (e.g. within 100 or 200 KeV), electric quadrupole excitation to the lowest 2^+ state may be the only available transition state. At energies at which electric dipole excitation becomes possible there will be a region of competition between $2^+(K=0)$ and $1^-(K=0)$ transition states. At slightly higher energies the principal contest should be between $1^-(K=0)$ and $1^-(K=1)$ states, etc. All three cases lead to distinctive angular distributions in photofission. The distribution becomes isotropic a few MeV above threshold owing to the large number and variety of accessible transition states, but reappears again at the threshold for second chance fission and again for higher chance fissions. Since the emission of a neutron from a primary excited state will again leave the residual nucleus in a condition with barely enough energy to fission, we may expect the spectrum of transition states (now

the low lying states of a deformed odd A nucleus) to determine the fragment angular distribution once again.

ELECTRON INDUCED FISSION

Suppose that measurements are made of the fission yield produced by scattering of electrons from ^{238}U or a similar target. The overall effect of the electrons on the target is assessed by comparing the electromagnetic field near the nucleus (at the origin of coordinates), produced by the scattering electron, with an equivalent field which could be produced by a pulse of radiation of external origin. In this way a virtual radiation spectrum is defined[12-14], but because the equivalent radiation is not a plane wave, it has a different composition from conventional incident radiation. The amount of electric quadrupole radiation, for example, is many times greater in virtual radiation than plane wave radiation[11]. Also there is no restriction on the magnetic substates of transferred angular momentum and as this is likely to effect the angular distribution rather drastically, we give here expressions for the virtual photon spectrum, for a given value of L, subdivided into the contributions of different M substates.

Using the notation of ref.(11) we consider the radiation field due to an electron moving in the Coulomb field of a charge Z. Since the electron enters along a specific direction $\underset{\sim}{p}_1$ we can write the initial wavefunction as a specific combination of partial wave solutions $\psi_{\kappa_1}^{m_1}$, denoted here by $\psi^{(+)}$:

$$\psi^{(+)}(\underset{\sim}{p}_1,\underset{\sim}{r}) = 4\pi\left(\frac{E_1+m_e}{2E_1}\right)^{1/2}\sum_{\kappa_1\mu_1} e^{i(\delta_{\kappa_1}+\ell_1\pi/2)}\, C(\ell_1\tfrac{1}{2}j_1;\mu_1-m_1,m_1)\cdot Y_{\ell_1}^{\mu_1-m_1}(\hat{p}_1)\,\psi_{\kappa_1}^{\mu_1}(p_1,r) \qquad (2)$$

where the electron quantum numbers E, p, κ, ℓ, j, μ and m acquire suffixes 1 or 2 to distinguish initial from final quantities.

The vector potential will be expressed in terms of the transverse electric and transverse magnetic multipole solutions, here denoted by

$$\underset{\sim}{A}^{(st)}_{\ell M}(\underset{\sim}{r},e) = \frac{-i}{\omega\sqrt{\ell(\ell+1)}}\ \underset{\sim}{\nabla}\times\left(\underset{\sim}{L}\, j_\ell(\omega r)\, Y_{\ell M}(\hat{r})\right)$$

and

$$\underset{\sim}{A}^{(st)}_{\ell M}(\underset{\sim}{r},m) = \frac{1}{\sqrt{\ell(\ell+1)}}\ \underset{\sim}{L}\, j_\ell(\omega r)\, Y_{\ell M}(\hat{r}) \qquad (3)$$

The label $^{(st)}$ is for <u>standing wave</u> solutions. We also need to use travelling wave solutions, in particular the <u>outgoing</u> solution labelled $^{(out)}$, which is obtained by replacing the spherical Bessel function $j_\ell(\omega r)$ by the spherical Hankel function $h^{(1)}_\ell(\omega r)$ in eqs.(2) and (3).

For an electron scattering from the initial state $\psi^{(+)}(\underset{\sim}{p}_1,\underset{\sim}{r})$ to a final state $\psi^{(-)}(\underset{\sim}{p}_2,\underset{\sim}{r})$, the electromagnetic potential produced at points in the neighbourhood of the origin will be

$$r\simeq 0,\ \underset{\sim}{A}(\underset{\sim}{r}) = \sum_{(\lambda)LM} \underset{\sim}{A}^{(st)}_{LM}(\omega,\underset{\sim}{r},\lambda)\int \psi^{(-)}(\underset{\sim}{p}_2,\underset{\sim}{r})^\dagger\ \underset{\sim}{\alpha}\cdot$$

$$\cdot\, A^{(out)*}_{LM}(\omega,\underset{\sim}{r},\lambda)\,\psi^{(+)}(\underset{\sim}{p}_1,\underset{\sim}{r})\, d^3r \qquad (4)$$

where $\underset{\sim}{\alpha}$ is the electron current operator.

Notice that $\underset{\sim}{A}^{(st)}_{LM}$ is the same field component as appears in the multipole expansion of a plane electromagnetic wave

$$\underset{\sim}{\varepsilon}_\mu e^{i\omega z} = \mu(2\pi)^{1/2}\sum_L (2L+1)^{1/2} i^L\left[\underset{\sim}{A}^{(st)}_{L\mu}(\omega,\underset{\sim}{r},M) + i\mu\,\underset{\sim}{A}^{(st)}_{L\mu}(\omega,\underset{\sim}{r},e)\right];\ \mu=\pm 1. \qquad (5)$$

where $\xi_{\pm 1} = \frac{1}{\sqrt{2}}(\hat{x} \pm i\hat{y})$ are the polarization vectors for the two states of circular polarization.

Provided that no discrimination is made on the basis of direction, i.e. the target and beam are not polarized, and there is no directional discrimination in detection of fission fragments or of the scattered electron, then the yield of excited states produced by virtual radiation can, for a given multipole transition, be related to the photoexcitation cross section σ_γ through a virtual photon spectrum[12-14]:

$$\sigma_e(E,\lambda,L) = \int \sigma_\gamma^{(\lambda L)}(\omega)\, N^{\lambda L}(E,\omega)\, d\omega/\omega \qquad (6)$$

The expression for $N^{\lambda L}$ we use is that given in ref.(11):

$$N^{(\lambda L)}_{(E_1,\omega)} = \frac{\alpha}{\pi}\frac{p_2}{p_1}\frac{(E_1+m_e)(E_2+m_e)\,\omega^4}{(2L+1)}$$
$$\times \sum_{K_1 K_2} S(\lambda)(2j_1+1)(2j_2+1)$$
$$\times \left| C(j_1 j_2 L; -\tfrac{1}{2}\ \tfrac{1}{2})\, R^{(\lambda)}(K_1, L, K_2)\right|^2 \qquad (7)$$

where it is understood that $E_2 = E_1 - \omega$, p_i is the electron momentum corresponding to energy E_i, and α is the fine structure constant. In eq.(7) $S(\lambda)$ is a projection operator which retains only those terms in the angular momentum sum satisfying the selection rule that $(l_1 + l_2 + L)$ must be even for $\lambda = e$ (electric multipole) and odd for $\lambda = m$ (magnetic multipole); $R^{(\lambda)}(K_1, L, K_2)$ is a radial integral defined in ref.(11)*.

If, on the other hand, we observe the angular distribution of emitted fragments, we are able to distinguish substates in the transition nucleus. Now the fact that

expression (4) contains a sum over all M-states, whereas eq.(5) contains only $M = \pm 1$, renders electron scattering and photon scattering non equivalent. The angular distribution for photofission via the transition state with quantum numbers L, K would be $W^{L}_{K1}(\theta)$, the corresponding distribution for electrofission is

$$W^{L}_{K}(\theta,E,\omega) = \sum_{M} W^{L}_{KM}(\theta)\, N^{\lambda LM}(E,\omega) \Big/ N^{\lambda L}(E,\omega) \qquad (8)$$

In eq.(8), $N^{\lambda LM}$ is the virtual photon spectrum broken down into the contributions of different M-states(as in figs.2 and 3), for which we find the expression

$$N^{\lambda LM}(E_1,\omega) = \frac{\alpha}{\pi}\,\omega^{4}\cdot\frac{p_2}{p_1}\cdot\frac{(E_1+m_e)(E_2+m_e)}{(2L+1)}\sum_{\mu=\pm\frac{1}{2}}\sum_{K_2}$$
$$\Big|\sum_{K_1} e^{i(\delta_{K_1}+\lambda_1\pi/2)}(2j_1+1)\,C(j_1 j_2 L;-\tfrac{1}{2}\,\tfrac{1}{2})\cdot$$
$$\cdot\, C(j_1 L j_2;\mu M)\,R^{\lambda}(K_1,L,K_2)\Big|^{2} \qquad (9)$$

where, of course,

$$\sum_{M} N^{\lambda LM}(E,\omega) = N^{\lambda L}(E,\omega) \qquad (10)$$

Expression (8) is distinguished from its counterpart for photofission, by being a function of E and ω as well as θ.

The quantities actually measured in practice are the fission yields as functions of energy and angle of emission, to obtain expressions for which it is necessary to integrate over the photon spectrum and sum over all undetermined quantum numbers. In a bremsstrahlung experiment, where the photon spectrum is denoted by $N_{Br}(E,\omega)$ (note that this is independent of multipole signature (λL)), the cross section measured is:

$$\frac{d\sigma_{B\gamma}(E,\theta)}{d\Omega} = \sum_{\lambda LK} W^{L}_{K1}(\theta) \int_{E_{th.}}^{E_0} \sigma_\gamma^{(\lambda LK)}(\omega)\, N_{B\gamma}(E,\omega)\, d\omega/\omega \qquad (11)$$

For electrons the angular distribution function must be included under the integral sign :

$$\frac{d\sigma_e(E,\theta)}{d\Omega} = \sum_{\lambda LK} \int_{E_{th.}}^{E_0} \sigma_\gamma^{(\lambda LK)}(\omega)\, W^{L}_{K}(\theta,E,\omega)\, N_e^{(\lambda L)}(E,\omega)\, d\omega/\omega \qquad (12)$$

Notice that the angular anisotropies persist only for energies a few MeV above threshold and thus the range E_{th} (threshold) to E_0 (electron kinetic energy) is very small and consequently the range over which we need to calculate functions of E and ω is very modest.

Analysis of an angular distribution does not proceed in any direct way, even for photofission, since there is no unique expansion of a function of θ in terms of $W^{L}_{K1}(\theta)$. Usually the expansion made is

$$\frac{d\sigma_{B\gamma}}{d\Omega} = a + b\sin^2\theta + c\sin^2 2\theta \qquad (13)$$

Any angular distribution created by dipole and quadrupole states can be expressed in this form. Clearly with three coefficients we must have no more than three states (L,K) contributing, e.g. (1,0), (1,1) and (2,0) to achieve an unique analysis. One might hope that the additional information provided by electron scattering would aid in the analysis to the point of being able to include a more complete set of quantum numbers. In principle, this is possible but, perhaps, not too realistic; we will devote a paragraph to it nevertheless.

Suppose that each angular distribution function

is analysed in the form of eq.(13) i.e.

$$W^{L}_{K1}(\theta) = a^{L}_{K}(E) + b^{L}_{K}(E)\sin^2\theta + c^{L}_{K}(E)\sin^2 2\theta \tag{14}$$

$$W^{\lambda L}_{K}(\theta, E, \omega) = a^{\lambda L}_{K}(E,\omega) + b^{\lambda L}_{K}(E,\omega)\sin^2\theta + c^{\lambda L}_{K}(E,\omega)\sin^2 2\theta \tag{15}$$

and we write, for convenience,

$$A^{KL}(E,\omega) = a^{L}_{K}(E)\, N_{Br}(E,\omega) \tag{16}$$

$$A^{\lambda LK}(E,\omega) = a^{\lambda L}_{K}(E,\omega)\, N^{(\lambda L)}_{e}(E,\omega) \tag{17}$$

The functions of eqs.(16) and (17) are accessible from theory. Now consider that each measured angular distribution is reduced to coefficients as in eq.(13), three for bremsstrahlung a, b, c, and three for electron induced fission a_e, b_e, c_e. We having then six equations derived from (11) and (12)

$$a(E) = \sum_{\lambda LK} \int \sigma_{\gamma}^{\lambda LK}(\omega)\, A^{KL}(E,\omega)\, d\omega/\omega \tag{18}$$

$$a_e(E) = \sum_{\lambda LK} \int \sigma_{\gamma}^{\lambda LK}(\omega)\, A^{\lambda LK}(E,\omega)\, d\omega/\omega \tag{19}$$

and counterpart equations for b, c, b_e, c_e. A simultaneous unfolding of eqs.(18),(19) and counterpart equations could, in principle, be performed to extract six cross sections $\sigma_{\gamma}^{\lambda LK}$; this unfortunately is not enough to cover all sets of quantum number λLK for dipole and quadrupole transitions (we hesitate to suggest it, but one could determine three more coefficients by positron scattering). More realistically, one might expect to use the much enhanced quadrupole spectrum in virtual radiation, and look at the

behaviour of $c_e(E)$ alone. It should be possible to analyse this in terms of isolated states of well defined K, for example, if such states exist. In the following section we will consider a few numerical examples.

DISCUSSION

Restricting ourselves to the three lowest collective band structures for an even-even transition nucleus (fig.1), we have shown (figs.4-6) the expected angular distributions of fission fragments following electro- and photo excitation for pure $L = 1, K = 0$; $L = 1, K = 1$ and $L = 2, K = 0$ levels. Although such pure transition states are not expected to be accessible in practice, these plots are nevertheless useful for the comparison purposes. The angular distributions have been plotted for a fixed value of photon energy, $E_\gamma = 6.5$ MeV, just above the fission threshold for ^{238}U. For electroexcitation, we have shown three different curves A, B and C corresponding to different incident (and scattered) electron energies chosen in such a way that the transferred virtual photon energy, ω, is always 6.5 MeV.

It can be seen clearly that the angular distributions are less anisotropic for electrofission as compared with those for photofission. Such behaviour is rather marked for the dipole case while not as pronounced for a quadrupole level. The anisotropy also seems to decrease with the increase in the incident electron energy (for fixed virtual photon energy). Virtual photons near the tip of the distribution produce the most pronounced angular distribution (i.e. are most like real photons). This is most apparent in figs. 2 and 3 which show the M = 1 component

dominating the spectrum in the tip region.

We have also shown the dependence of the corresponding angular distribution coefficients (analysed as in eqs. (14) and (15)) on the incident electron energy in figs. 7-9. It is apparent, that, although it is possible to analyse any angular distribution data in terms of eq.(13), the energy dependence of the resulting coefficients cannot be ignored in the case of virtual photons.

FOOT NOTE FOR PAGE 6.

* The gauge used here (transverse) is different from that used in this reference[11] but the expression for $R^{(\lambda)}$ can be rendered in the same form with proper subtraction of the pole at the origin encountered in the transverse gauge.

The assistance and hospitality of the staff of Instituto de Física, Universidade de São Paulo, and its director Professor José Goldemberg are most gratefully acknowledged, also a travel grant to one of us (DSO) from Conselho Nacional de Desenvolvimento Científico e Tecnológico is gratefully acknowledged.

REFERENCES

1) A. Bohr, in Proceedings of the International Conference on the Peaceful uses of Atomic Energy, Geneva 1955 (United Nations, New York 1956) Vol.2, P.151.

2) J.J.Griffin, Phys. Rev. 116(1959) 107.

3) J.R.Huizenga, in Proceedings of International Nuclear Physics Conference, Edited by Becker, Goodman, Stelson and Zucker; P.721, Academic Press, New York (1967).

4) J.R.Huizenga, Nucl. Technology 13 (1972) 20.

5) J.R.Huizenga and H.C.Britt, in Proceedings of International Conference on Photonuclear Reactions and Applications, Asilomar; Edited by B.L.Berman, Lawrence Livermore Laboratory 2 (1973) 833.

6) R. Vandenbosch and J.R.Huizenga, Nuclear Fission, Academic Press, New York,1973.

7) P. Rasch, G.Fiedler and E. Konecny, Nucl. Phys.A219(1974)397.

8) U. Kneissl, G.Kuhl and A. Weller, Phys. Lett.49B (1974) 440.

9) U.Kneissl, G.Kuhl, K.H.Leister and A. Weller, Nucl. Phys. A256 (1976) 11.

10) J.D.T. Arruda Neto, S.B.Herdade, B.S.Bhandari and I.C.Nascimento, In print in Phys. Rev. C.

11) W.W.Gargaro and D.S.Onley, Phys. Rev. C4 (1971) 1032.

12) C.F.Weizacker, Z. Phys. 88 (1934) 612.

13) E.J.Williams, Kgl. Dansk. Vid. Selsk. 13, No.4(1935).

14) R.H.Dalitz and D.R.Yennie, Phys. Rev. 105 (1957) 1598.

15) V.M.Strutinsky, Nucl. Phys. A95 (1967) 420.

FIGURE CAPTIONS

Fig. 1: Schematic diagram of possible collective band structure for an even-even transition nucleus with a stable quadrupole deformation. The energy scale is schematic only (from ref.(3)).

Fig. 2: Virtual photon spectrum for E1 radiation from a 10 MeV electron scattering from a nucleus of charge, z = 92, showing contributions of substates M = 0 and M = 1 (the sum of both M = +1 and -1).

Fig. 3: Virtual photon spectrum for E2 radiation from a 10 MeV electron scattering from a nucleus of charge 92, showing M = 0, 1 and 2 contributions.

Fig. 4: Fission fragment angular distribution expected for a pure L = 1, K = 0 level in photo and electroexcitation. The solid curve represents photofission angular distribution while the dashed curves represent electrofission angular distributions for electron energies of (A) 7.5 MeV, (B) 9.5 MeV, and (c) 11.5 MeV.

Fig. 5: Fission fragment angular distribution expected for a pure L = 1, K = 1 level in photo- and electroexcitation. Different curves have the same meaning as in Fig.(4).

Fig. 6: Fission fragment angular distribution expected for a pure L = 2, K = 0 level in photo- and electroexcitation. Different curves have the same meaning as in Fig.(4).

Fig. 7: Behaviour of angular distribution coefficients versus incident electron energy for a pure L = 1, K = 0 level.

Fig. 8: Behaviour of angular distribution coefficients versus incident electron energy for a pure L =1, K =1 level.

Fig. 9: Behaviour of angular distribution coefficients versus incident electron energy for a pure L = 2, K = 0 level.

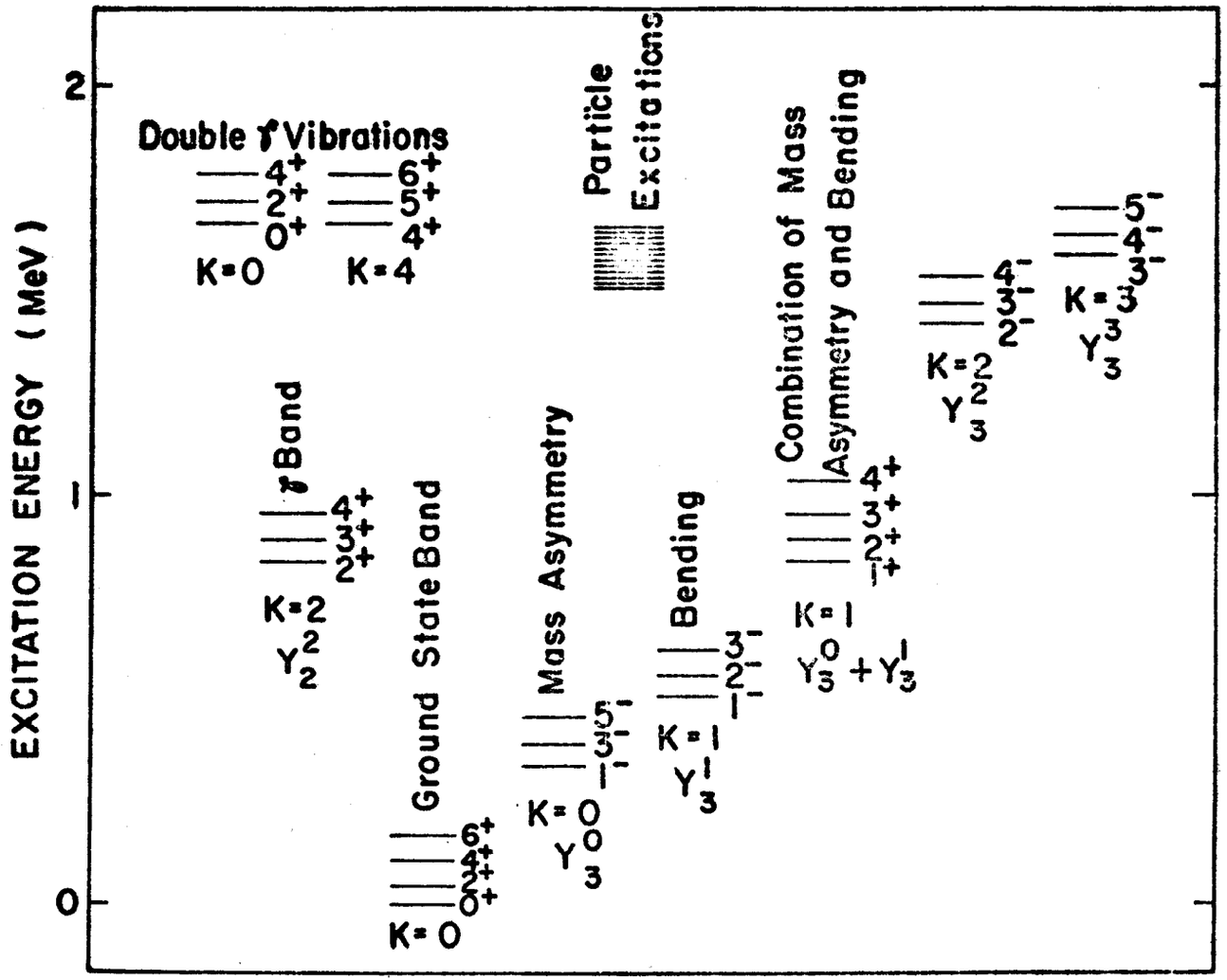
EXCITATION ENERGY (MeV)
2
1
0
Double γ Vibrations
4+
2+
0+
K=0
6+
5+
4+
K=4
Particle
Excitations
γ Band
4+
3+
2+
K=2
Y 2 2
Ground State Band
6+
4+
3+
2+
0+
K=0
Mass Asymmetry
5-
3-
1-
K=0
Y 3 0
Bending
3-
2-
1-
K=1
Y 3 -1
Combination of Mass
Asymmetry and Bending
4+
3+
2+
K=1
Y 3 0 + Y 3 1
4-
3-
2-
K=2
Y 3 2 2
5-
4-
3-
K=3
Y 3 3

Fig. 1

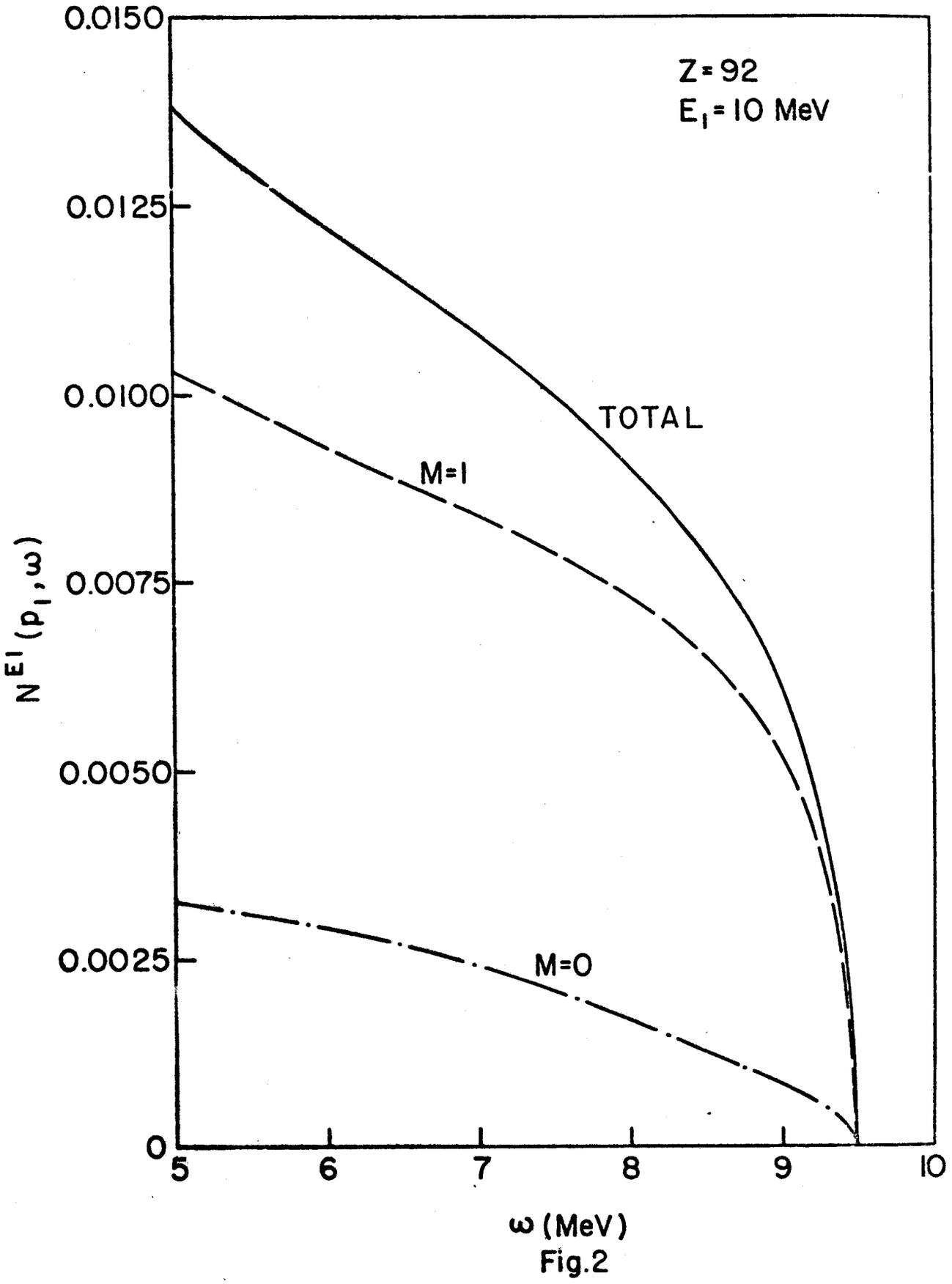
0.0150
0.0125
0.0100
0.0075
0.0050
0.0025
0
5
6
7
8
9
10
Z = 92
E1 = 10 MeV
TOTAL
M=1
M=0
N^E1 (p1, ω)
ω (MeV)

Fig.2

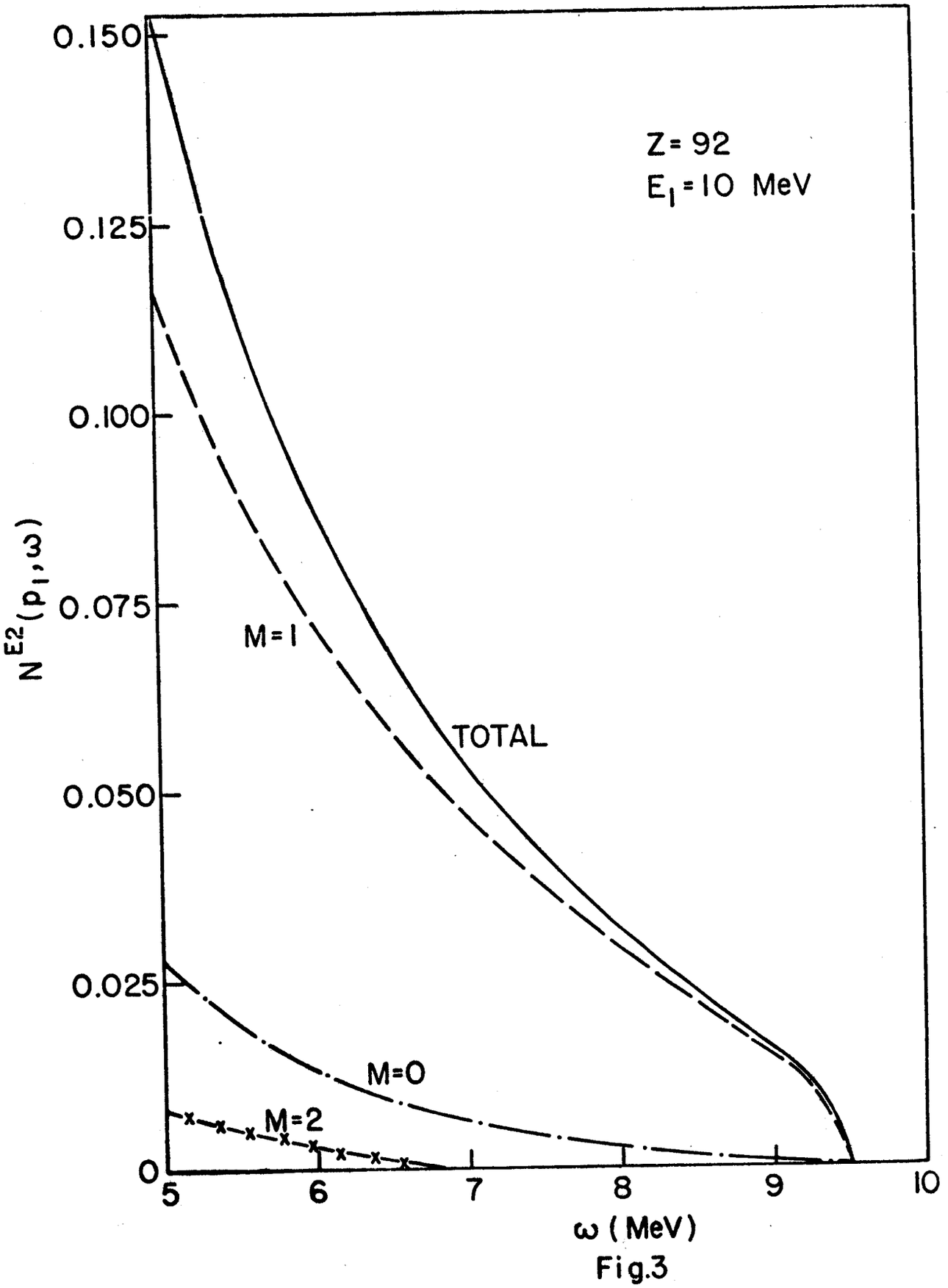
Z= 92
E1 = 10 MeV
0.150
0.125
0.100
0.075
0.050
0.025
0
N^E2(p1, ω)
M=1
TOTAL
M=0
M=2
5
6
7
8
9
10
ω (MeV)

Fig.3

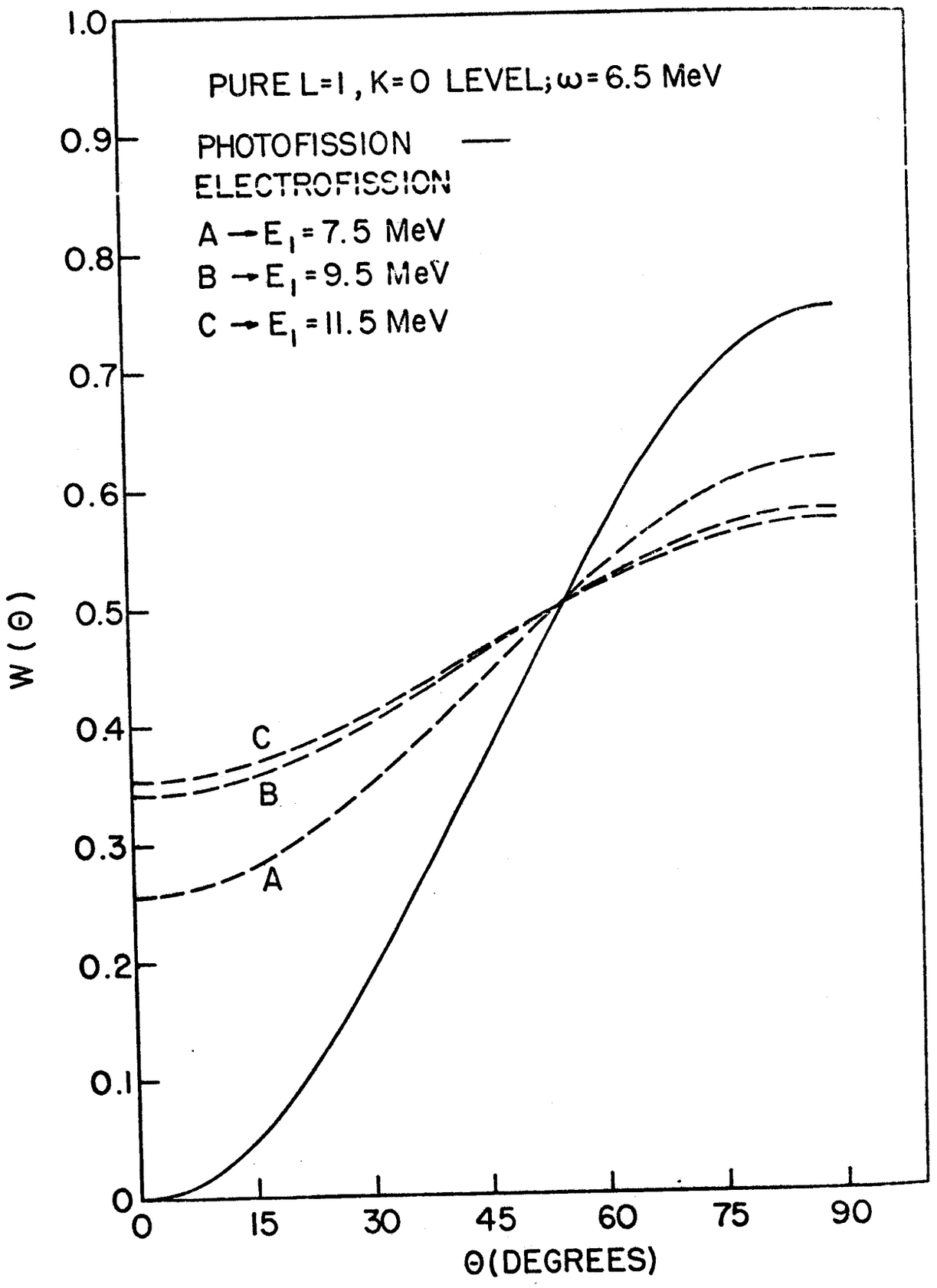
PURE L=1, K=0 LEVEL; ω=6.5 MeV
PHOTOFISSION
ELECTROFISSION
A → E1 = 7.5 MeV
B → E1 = 9.5 MeV
C → E1 = 11.5 MeV
W(Θ)
Θ(DEGREES)
0
0.1
0.2
0.3
0.4
0.5
0.6
0.7
0.8
0.9
1.0
0
15
30
45
60
75
90
A
B
C

Fig. 4

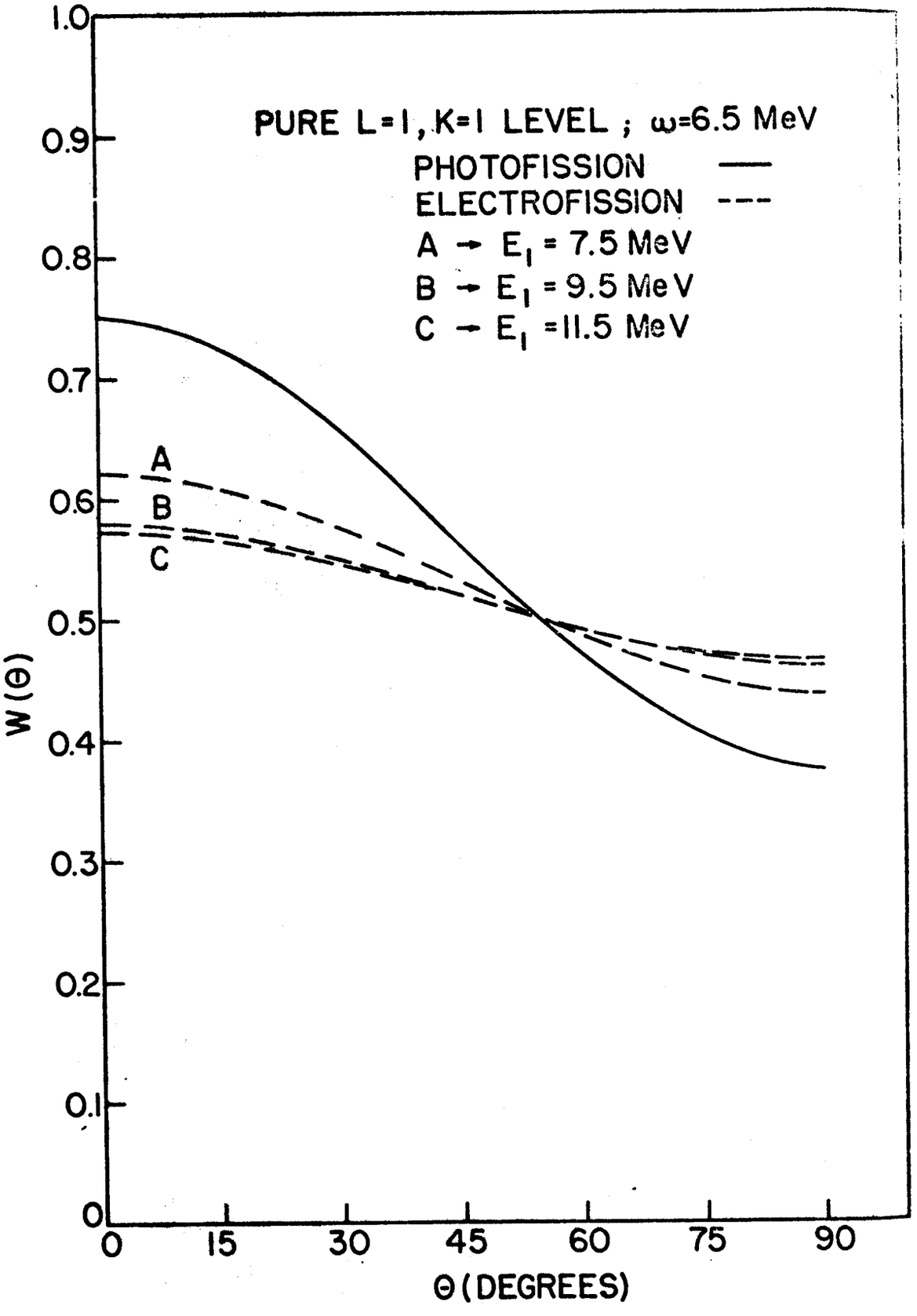
PURE L=1, K=1 LEVEL ; ω=6.5 MeV
PHOTOFISSION
ELECTROFISSION
A → E1 = 7.5 MeV
B → E1 = 9.5 MeV
C → E1 = 11.5 MeV
A
B
C
W(Θ)
1.0
0.9
0.8
0.7
0.6
0.5
0.4
0.3
0.2
0.1
0
0
15
30
45
60
75
90
Θ (DEGREES)

Fig.5

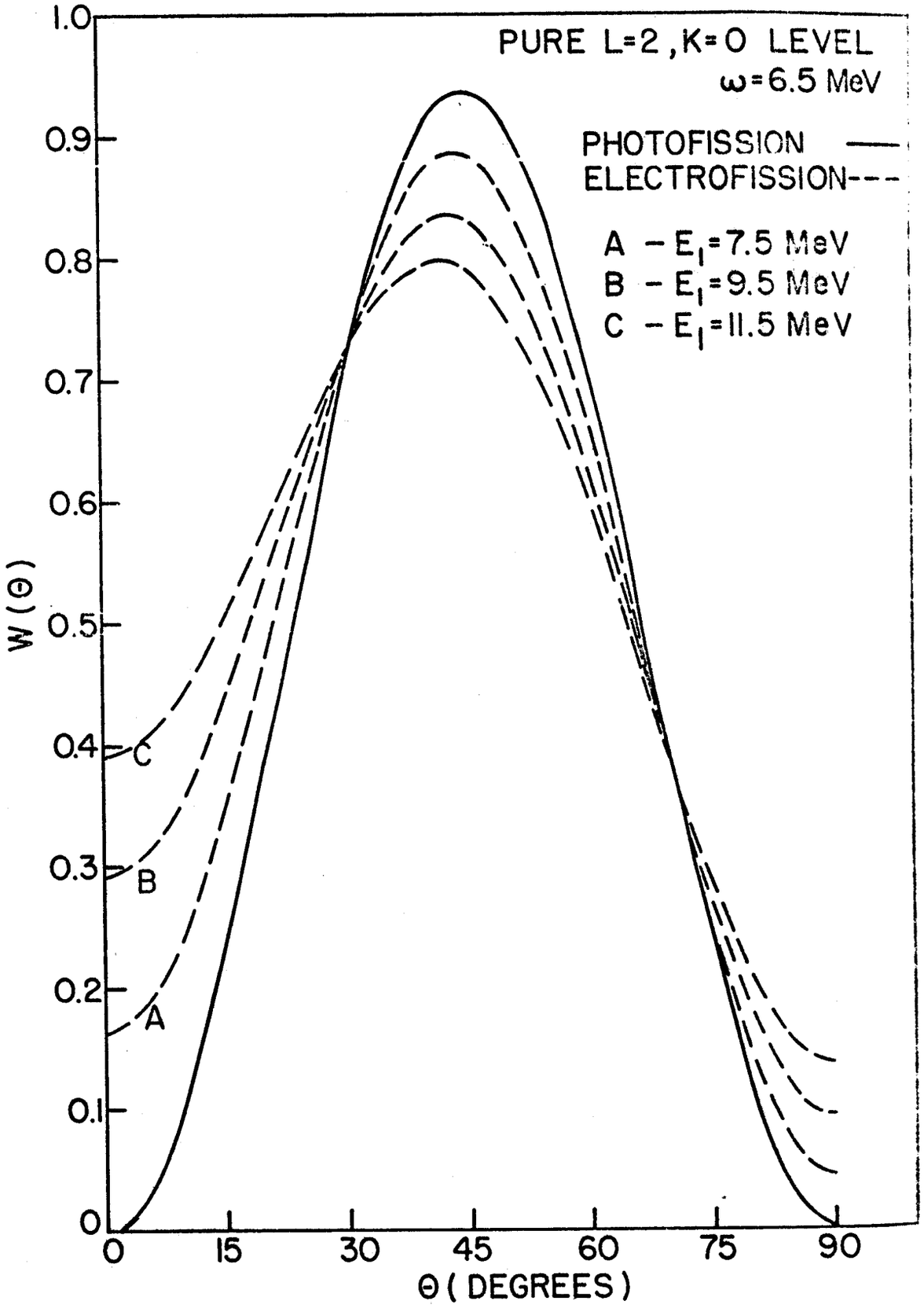
PURE L=2, K=0 LEVEL
ω=6.5 MeV
PHOTOFISSION ——
ELECTROFISSION---
A – E1=7.5 MeV
B – E1=9.5 MeV
C – E1=11.5 MeV
W(Θ)
Θ (DEGREES)
1.0
0.9
0.8
0.7
0.6
0.5
0.4
0.3
0.2
0.1
0
0
15
30
45
60
75
90
A
B
C

Fig.6

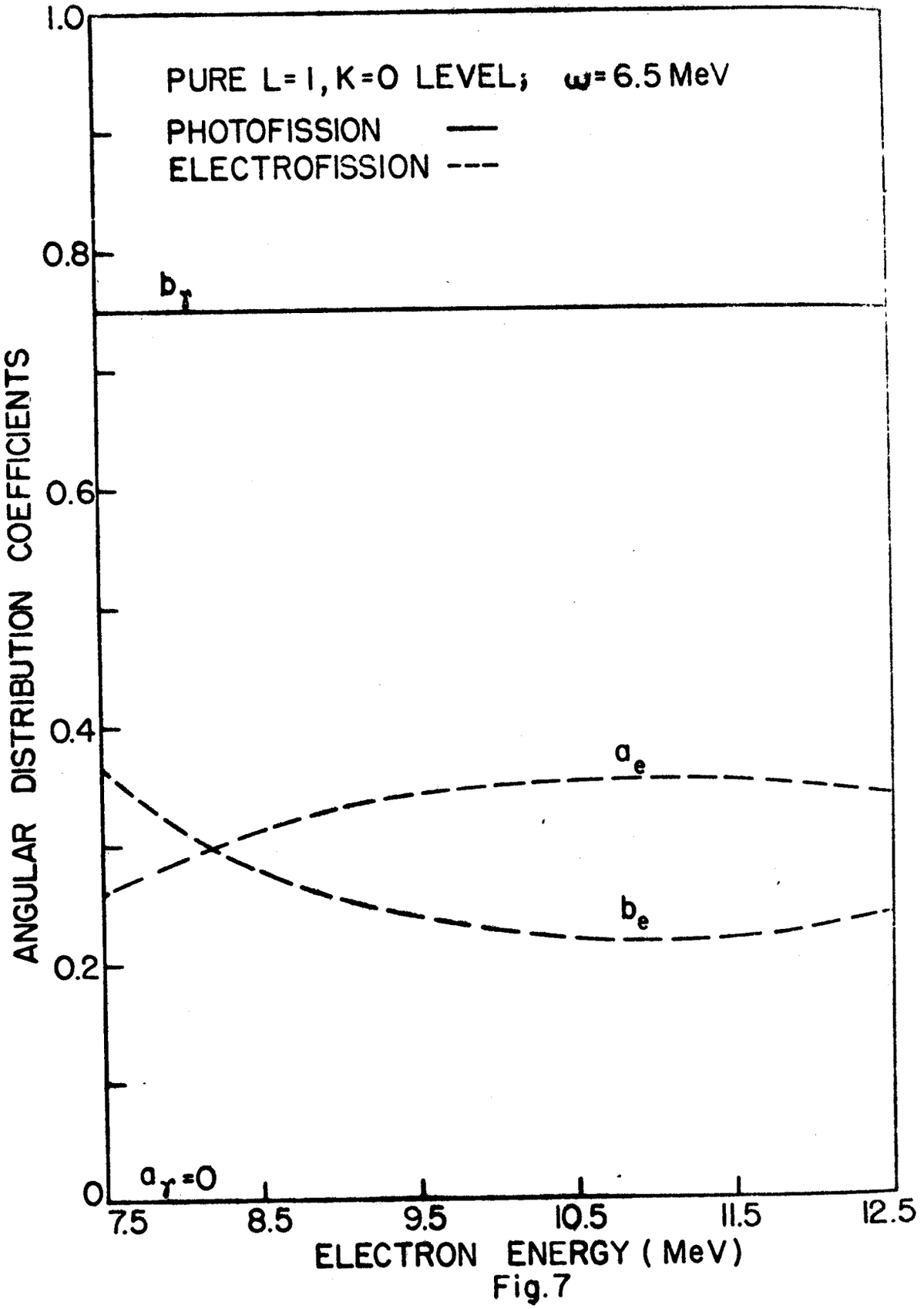
PURE L=1, K=0 LEVEL; ω=6.5 MeV
PHOTOFISSION
ELECTROFISSION
1.0
0.8
0.6
0.4
0.2
0
b_γ
a_e
b_e
$a_\gamma=0$
ANGULAR DISTRIBUTION COEFFICIENTS
7.5
8.5
9.5
10.5
11.5
12.5
ELECTRON ENERGY (MeV)
Fig. 7

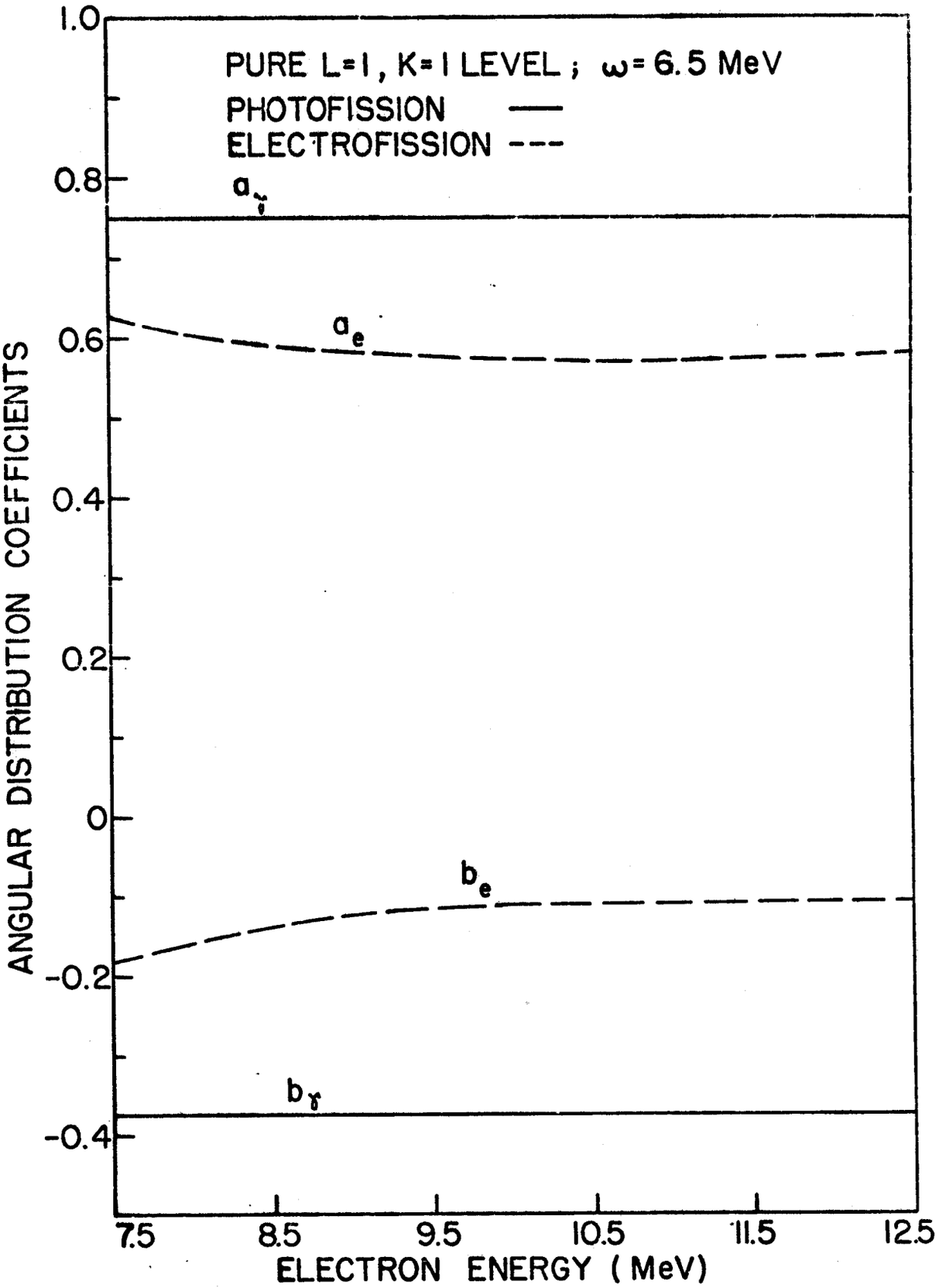
PURE L=1, K=1 LEVEL ; ω= 6.5 MeV
PHOTOFISSION
ELECTROFISSION
a_γ
a_e
b_e
b_γ
ANGULAR DISTRIBUTION COEFFICIENTS
1.0
0.8
0.6
0.4
0.2
0
-0.2
-0.4
7.5
8.5
9.5
10.5
11.5
12.5
ELECTRON ENERGY (MeV)

Fig. 8

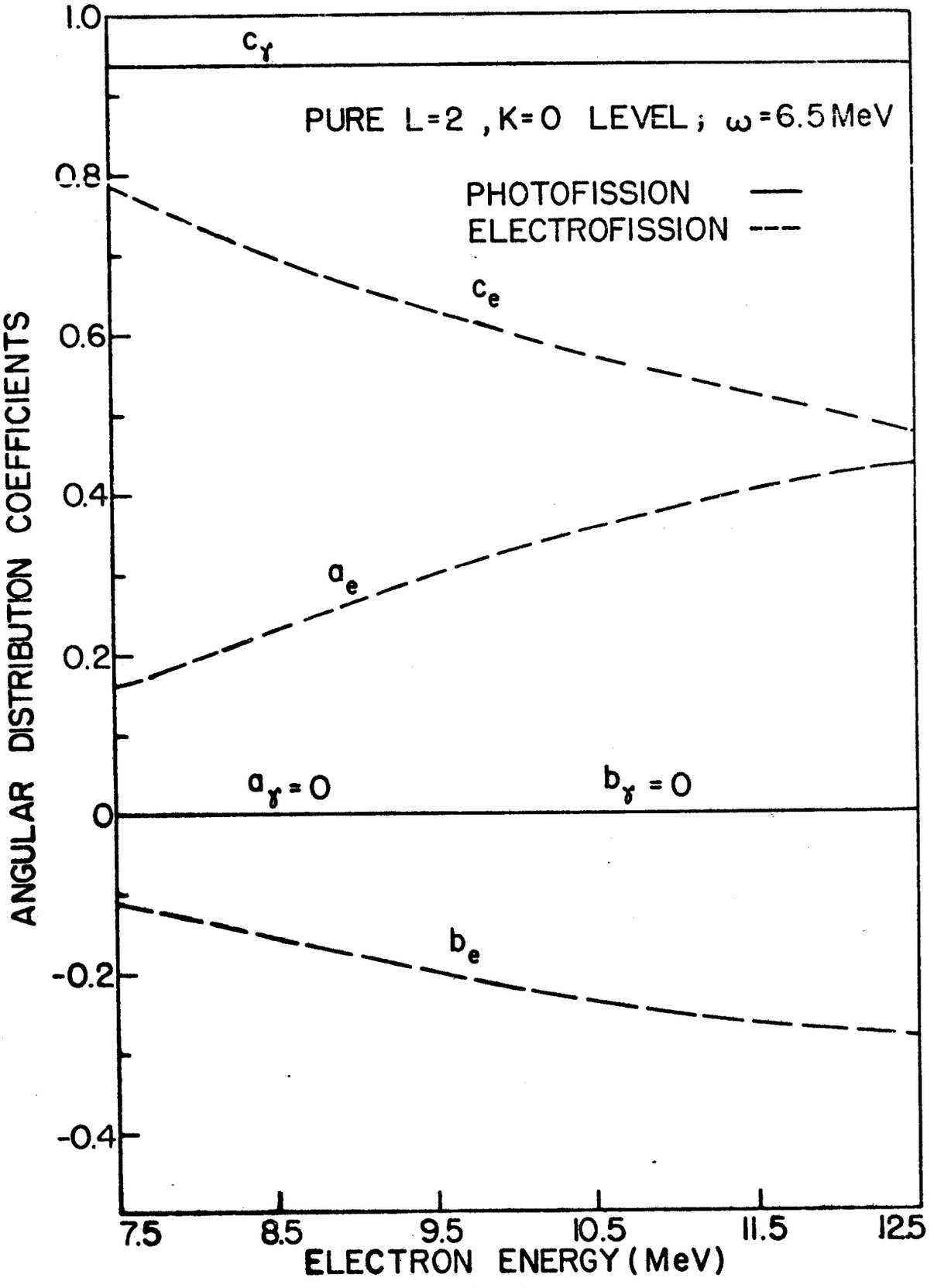
1.0
0.8
0.6
0.4
0.2
0
-0.2
-0.4
c_γ
PURE L=2 , K=0 LEVEL ; ω=6.5 MeV
PHOTOFISSION
ELECTROFISSION
c_e
a_e
$a_\gamma = 0$
$b_\gamma = 0$
b_e
ANGULAR DISTRIBUTION COEFFICIENTS
7.5
8.5
9.5
10.5
11.5
12.5
ELECTRON ENERGY (MeV)

Fig. 9